Better understanding of the role of SiO2, P2O5 and Al2O3 on the spectroscopic properties of Yb 3+ doped silica sol-gel glasses

Benoit Glorieux, Turkka Salminen, Jonathan Massera, Mika Lastusaari, Laeticia Petit

Better understanding of the role of SiO_2, P_2O_5 and Al_2O_3 on the spectroscopic properties of Yb^{3+} doped silica sol-gel glasses

Benoit Glorieux[1], Turkka Salminen[2], Jonathan Massera[3], Mika Lastusaari[4,5], Laeticia Petit[2*]

[1] *CNRS, Université de Bordeaux, ICMCB, 87 Avenue du Dr Schweitzer, F-33608 Pessac, France*

[2] *Laboratory of Photonics, Tampere University of Technology FI-33101 Tampere, Finland*

[3] *BioMediTech, University of Tampere and Tampere University of Technology, Biokatu 10/FI-33520 Tampere, Finland*

[4] *University of Turku, Department of Chemistry, FI-20014 Turku, Finland*

[5] *Turku University Centre for Materials and Surfaces (MatSurf), Turku, Finland.*

* *Correspondence to laeticia.petit@tut.fi*

Abstract

Yb^{3+} doped silica sol-gel glass powders were prepared with different concentrations of SiO_2, Al_2O_3 and P_2O_5 in order to understand the impact of the glass composition on the Yb^{3+} emission properties. In this paper, we clearly show that not only the Al/P ratio but also the SiO_2 content have an impact on the Yb^{3+} spectroscopic properties. Our results provide new insight on the real impact of the composition on the spectroscopic properties of Yb^{3+} doped sol-gels: we demonstrate that an increase in the Al_2O_3 content at the expense of P_2O_5 leads to an increase in the intensity of the emission at 1000nm of the Yb^{3+} ions whereas an increase in the SiO_2 content decreases it. We clearly showed that the inexpensive sol-gel approach can be easily used when investigating new Yb^{3+} doped silica glasses.

Introduction

In recent years, the demand for high-power fiber lasers and laser processing has led to increased research on Yb^{3+}-doped silica glasses [1-3]. Intense efforts are on-going, worldwide, in order to increase the performance of the Yb-doped silica glasses. Generally, a high Yb concentration is necessary to reach sufficient pump absorption, to reduce the fiber length and to increase the threshold for undesirable nonlinear effects in fibers [4].

To prevent Yb clustering from occurring when using high Yb concentration, Al_2O_3 or P_2O_5 are added in the silica glass [5]. The simultaneous combination of these two oxides present an interesting cooperative behavior: the rare-earth dissolution in the ternary Al_2O_3-P_2O_5-SiO_2 host systems was found to be higher than in the binary P_2O_5-SiO_2 or Al_2O_3-SiO_2 glasses [6]. Although the refractive index (RI) of silica glasses increases with the addition of Al_2O_3 or P_2O_5, the simultaneous combination of Al_2O_3 and P_2O_5 leads to the formation of a glass with a lower RI than that of silica. This low RI was related to the formation of $AlPO_4$ units in the glass network [7]. This combination of Al_2O_3 and P_2O_5 offers the possibility of doping the fibre core with higher rare-earth content while maintaining a relatively low RI. The influence of P^{5+} on the absorption cross section of Yb^{3+} in Al_2O_3-P_2O_5-SiO_2 glass fiber was reported in [8]. A core composition with equal content of Al and P was found to be the most promising to achieve Yb fibers with low photodarkening, high laser efficiency and low numerical aperture of the fiber despite of the high codoping. For this study, the preforms were prepared by MCVD (Modified Chemical Vapor Deposition) and solution doping according to a route with carefully controlled process steps.

Sol–gel method has been now used to prepare high SiO_2-containing glasses and fibers. Compared with the traditional MCVD method, this technique has the advantage to allow the preparation of silica glasses at a low synthesis temperature [9]. Additionally, glass samples with a broad composition range can be prepared in large sizes. Finally, Al_2O_3 and P_2O_5 can be easily and homogeneously incorporated onto SiO_2 glass [5]. There are few reports about using

sol–gel method to prepare silica fiber preform. Wang et al investigated the influence of Al^{3+} and P^{5+} ion contents on the valence state of Yb^{3+} ions and the dispersion effect of Al^{3+} and P^{5+} ions on Yb^{3+} ions in silica glass [10]. They found that with increasing Al^{3+} or P^{5+} ion content in Yb^{3+}-doped silica glass, the Yb^{3+}/Yb^{2+} redox process can be greatly accelerated. Reduction in the emission intensity of Yb^{3+} was observed, especially at the high P^{5+}/Al^{3+} molar ratio region. Xu et al. reported the mechanism of the decrease in Yb^{3+} absorption and emission cross sections in Al_2O_3-P_2O_5-SiO_2 glass caused by P^{5+} doping [11]: Yb^{3+} coordinates to the P–O site in glass with molar ratio of $P^{5+}/Al^{3+} < 1$, and coordinates to the P = O site in glass with molar ratio of $P^{5+}/Al^{3+} > 1$. This change decreases the Yb^{3+} asymmetry degree and thus leads to the decline in Yb^{3+} absorption and emission cross sections. However, in both studies [10-11], the authors discussed the influence of Al^{3+} and P^{5+} ion contents on the spectroscopic properties of Yb^{3+} ions although the concentration of the SiO_2 varied between ~86 and 96 mol% as the Al_2O_3/P_2O_5 ratio was changed.

In this paper, new sol-gel glass powder with different SiO_2, Al_2O_3 and P_2O_5 concentrations were prepared in order to better understand the role of SiO_2, P_2O_5 and Al_2O_3 on the Yb^{3+} emission properties.

Sample preparation and characterization

Tetraethoxysilane (TEOS) (Sigma Aldrich, 98%), C_2H_5OH, $AlCl_3$-$6H_2O$ (Sigma Aldrich, 97%), H_3PO_4, and $YbCl_3$-$_6H_2O$ (Sigma Aldrich, 99.9%) were used as precursors. Deionized water was added to sustain the hydrolysis reaction. The pure analytical-grade chemical reagents were weighed according to the molar composition of samples listed in Table 1. Sol-gels glasses with SiO_2 content ranging from 91.8 to 97.8mol% were prepared with 0.2mol% of Yb_2O_3 and different Al_2O_3/P_2O_5 ratios (x). All precursors were thoroughly stirred at 50 °C for a day to form homogeneous doping sols. The above sols were then heated at 850

°C for 6h and then at 1100ºC for 1h to produce glasses, in which organics and hydroxyl are decomposed [12]. The sol-gels were finally crushed into powders.

The composition of the sol-gel glasses was checked by using a Scanning Electron Microscope (Leo 1530 Gemini, Zeiss) coupled with an Energy Dispersive X-Ray Analyser (SEM/EDXA) (Vantage by Thermo Electron Corporation).

The IR emission spectra were measured with an Edinburgh Instruments monochromator (M300) and a liquid nitrogen cooled germanium detector (ADC 403L) at room temperature using a UV excitation source and also an excitation source emitting at 980 nm. The measurement of the visible emission spectra was performed using a setup for regular photoluminescence and one for up-conversion. The photoluminescence was measured with a Varian Cary Eclipse Fluorescence Spectrophotometer equipped with a Hamamatsu R928 PMT (photomultiplier) and a 15 W xenon lamp. The up-conversion luminescence spectra were measured with an Avaspec-HS-TEC CCD spectrometer at room temperature. The materials were excited with an Optical Fiber Systems IFC-975-008 NIR laser (6 W; λ_{exc} **= 974 nm**). Emission was collected at a 90° angle to the excitation and directed to the detector with an optical fiber (diameter: 600 µm). In the excitation path, a long-pass filter with a cutoff at 900 nm (Edmund Optics) was used to ensure a pure NIR excitation. In the emission light path, an extended hot mirror filter (Edmund Optics) with a good transmission at visible wavelengths was used to exclude the scattered excitation radiation. Same amount of sol-gel powder was used for the emission spectra measurement to be able to compare the intensity of the emission.

The Raman spectra were recorded using a 532 nm wavelength laser (Cobolt Samba) for excitation and measured with a 300 mm spectrograph (Andor Shamrock 303) and a cooled CCD camera (Andor Newton 940P). All spectra are normalized to the band showing the maximum intensity.

Results and discussion

In order to understand the real impact of SiO_2, Al_2O_3 and P_2O_5 on the Yb^{3+} spectroscopic properties, sol-gel glass powders were prepared with various Al_2O_3/P_2O_5 ratios (x) ranging from 0.3 to 3.3 and various SiO_2 concentrations ranging from 91.8 to 97.8mol%. Table 1 lists the composition of the different investigated sol-gel glasses.

Figure 1a show the normalized emission properties of the sol-gel glass powders prepared with Al_2O_3/P_2O_5 ratio of 0.8 and a concentration of SiO_2 ranging from 91.8 to 97.8mol%. The spectra exhibit broad bands around 1000 nm which are typical of Yb^{3+} emission ($^2F_{5/2}\rightarrow{}^2F_{7/2}$) bands in silica glass, the shape of which is not strongly impacted by different SiO_2 contents [10-11]. However, as depicted in Figure 1b, an increase in the SiO_2 content decreases the emission intensity at 1µm of the sol-gels with x=0.8 (P-rich) and 1.25 (Al-rich). This can be related to concentration quenching due to the well-known low solubility of Yb^{3+} in silica glass: the concentration quenching is related usually to the conjunction of rare-earth (RE) ions clustering through RE-O-RE bonds with energy transfer between the clusters by a cross-relaxation mechanism or phonon-assisted energy transfer as reported in [13, 14]. A larger decrease of the emission at 1µm is observed in the Al-rich sol-gel (x=1.25) than in the P-rich sol gels (x=0.8) when the content of SiO_2 increases from 91.8 to 97.8 mol% probably due to different Yb^{3+} sites in the sol-gels: the second neighbor shell of Yb^{3+} is suspected to be mainly constituted of P atoms in P-rich sol-gels whereas it is composed of a mixture of Al and Si second neighbors. Therefore an increase in the SiO_2 content is suspected to strongly modify the site of Yb^{3+} in the Al rich sol-gels and so the intensity of the emission at 1µm.

Figures 2 show the up-conversion emission spectra of the sol-gel powders under 974 nm excitation. The band at 325 nm is the third harmonic of the excitation wavelength, which is generated inside the detector because the excitation at 974 nm cannot be completely blocked

from the detector by the filter used. The shoulder at ~350 nm could be due to the signal from the $^3P_0 \rightarrow {}^3F_4$ transitions of Tm^{3+}, which is a common impurity in Yb-containing compounds [16]. Another common impurity in Yb-containing compounds, which is even more effective in up-conversion, is Er^{3+}. The lines at 526, 550 and 660 nm can be related to the $^2H_{11/2} \rightarrow {}^4I_{15/2}$, $^4S_{3/2} \rightarrow {}^4I_{15/2}$ and $^4F_{9/2} \rightarrow {}^4I_{15/2}$ transitions of Er^{3+}, respectively [16]. Between 450 and 530 nm is the band of Yb^{3+} co-operative emission [15, 17]. The intensity of this band is far weaker compared to the intensity of the Er^{3+} impurity lines, although the concentration of Yb^{3+} is much higher than that of the Er^{3+}. This is due to the relative efficiency of the co-operative luminescence, which is five orders of magnitude lower than that of the regular energy transfer up-conversion as explained in [17]. With increasing the SiO_2 content, the up-conversion emission signals from the sol-gels with x=0.8 increase (Figure 2a), whereas there is a slight decrease in the intensity of the emission bands from the sol-gels with x=1.25 (Figure 2b). This shows that the P-rich network is more sensitive to the changes in the sol-gel compositions than the Al-rich network probably due to the fact that phosphorus is completely miscible in silica [7]. As explained earlier, the second neighbor shell of Yb^{3+} is suspected to be mainly constituted of P atoms in the P-rich sol gels. Therefore, we think that an increase in SiO_2 content in the P-rich sol gels reduces the distance between Yb^{3+} ions increasing the intensity of the Yb^{3+} co-operative emission.

Figures 3 exhibit the visible emission spectra under 255nm excitation, which corresponds to the maximum of the Yb-O charge transfer band [18]. The spectra show broad bands at ~400, ~500 and in the 600-700nm range, which have previously been attributed to, respectively, oxygen deficiency center (II) (ODC(II)) and E' center [19], hydrogen-related species and non-bridging oxygen hole centers (NBOHCs) [20]. The band at ~400nm could be also related to phosphate-relate oxygen hole centers (POHC) according to [21] and the main band at ~500nm could be related to the emission of Yb^{2+} and to $[AlO_4]^0$ centers [22]. The blue (410 nm) and

red (660 nm) bands are, also, very typical of the emission of Ti^{3+} species in Al_2O_3 [23] and titanium is a frequent impurity in materials with Al. Titanium is a very efficient emitter capable of giving luminescence even in ppm concentrations [23]. The presence of titanium may also create the redox pairs $Ti^{3+/4+}/P^{3+/5+}$ and $Ti^{3+/4+}/Yb^{2+/3+}$. An increase of the SiO_2 content has no real impact on the intensity (at ±10%) of the bands at 500nm and in the 600-700nm region in both sol-gel systems (x=0.8 and 1.25) but it increases the intensity of the band at 400nm which is an indication of an increase in ODC (II) and E' center concentrations. The spectra of the P-rich sol-gels exhibit the emission band at 400nm with higher intensity than those of Al-rich sol-gels for same SiO_2 content indicating the presence of a larger number of ODC (II) and E' in the P-rich sol-gels than in the Al-rich sol-gels.

Based on the spectroscopic properties of the Yb^{3+} doped sol-gel powders presented in Figures 1 to 3, it is clear that a change in the SiO_2 content has an impact on the Yb^{3+} spectroscopic properties due to its impact on the Yb^{3+} coordination sites and on the Yb-Yb distance. Therefore, in order to understand the real contribution of Al_2O_3 and P_2O_5 on the spectroscopic properties of Yb^{3+}, sol-gel glass powders were prepared with a constant SiO_2 concentration (95.8mol%) and with a Al/P ratio ranging from x=0.3 to 3.3.

Figures 4 depict the emission properties of the sol-gels as a function of x. As seen in Figure 4a, an increase in x leads to an increase in intensity of the emission at 1µm. Similar results were observed in [10]. As depicted in Figure 4b, the shape of the emission band is slightly modified when x increases indicating that the Al and P atoms participate to the second coordination shell around the Yb^{3+} ions: as explain in the previous paragraph, the second neighbor shell of Yb^{3+} is suspected to be mainly constituted of P atoms in the P-rich sol-gels whereas a mixture of Al and Si are thought to be the second neighbors in the Al-rich sol-gels.

Therefore, we suspect an increase in the asymmetric degree of the coordination sites of Yb^{3+} and so an increase in the emission at 1µm when x increases.

Figure 5 shows the up-conversion emission spectra of the sol-gel powder as a function of the x under 974 nm excitation. The spectra exhibit similar peaks than those seen in Figures 2. The co-operative emission of Yb^{3+} increases with increasing x clearly indicating that an excess in Al promotes Yb-Yb pair formation and thus the probability of the co-operative emission of Yb^{3+} increases whereas an excess in P increases the solubility of Yb in the glass host [15]. One can also notice a decrease in the Er^{3+} and Tm^{3+} (as seen by the increase of the intensity of the band at 320nm as compared to that of 350nm) emissions with an increase of x. This can be related to the increase in OH content as discussed when analyzing the Raman spectra presented in Figure 7.

Figure 6 shows the visible emission spectra under 255nm excitation. The spectra show broad bands at ~400, ~500 and in the 600-700nm range. One can observe a reduction in intensity of the band at 400nm with an increase in x probably due to the reduction in the P_2O_5 content which is expected to reduce the POHC defects. It is interesting to point out that the sol-gels with x=0.3 and 1 exhibit a band at 500nm with similar intensity (at ±10%) while the other sol-gels exhibit this band with higher intensity. This band can be related to hydrogen-related species, $[AlO_4]^0$ centers but also to the emission of Yb^{2+}. Therefore, it is possible to think that an increase in the Al_2O_3 at the expense of P_2O_5 increases the hydrogen species, $[AlO_4]^0$ centers and also the Yb^{2+} content as suggested in [11]. At x=1, $AlPO_4$ are expected to form at the expense of AlO_4 units leading to a reduction in intensity of the band at 500nm. Except for the sol-gel with x=0.8, there is no impact of x on the intensity of the bands at >600nm, related to NBOHCs.

In order to understand the impact of the Al_2O_3/ P_2O_5 ratio on the Yb^{3+} spectroscopic properties of the sol-gel powder, the Raman spectra of the investigated sol-gel powders were

measured. They are presented in Figure 7. The spectra consist of bands around 400, 600, 800 and 1100cm^{-1} that agree with the spectra reported in the literature. The main optical modes of the Si–O–Si group can be assigned as follows: (i) Si–O–Si asymmetric stretching at 1000–1200 cm^{-1} related to Q^4 groups, composed of sites with three- and four-fold rings, (ii) the shoulder at 750 cm^{-1} is attributed to bending vibration, and (iii) the rocking vibration is identified at 560–620 cm^{-1} [24-25]. The strong band appearing at 400 cm^{-1} can be associated with the symmetric stretching Si – O – Si bond vibration. The presence of the shoulders at 485 and 600 cm^{-1}, labeled as so-called defects lines D1 (four-membered rings) and D2 (three-membered rings) respectively, reveal the existence of ring structures in the glass network. These features have been interpreted by Galeener et al. [25] as the signature of the symmetric stretch of regular fourfold and planar threefold ring structures embedded in the more irregular glass network. The 800 cm^{-1} band is due to the O – Si – O symmetric stretch vibration [26]. The shoulder at ~1200cm^{-1} can be related to the NBO species as suggested in [27]. The band from 900 to 970 cm^{-1} with a small intensity which can be seen only in some spectra can be associated with Si-NBO stretching and the very weak band near 980cm^{-1} to Si–OH stretching [9,12].

Given the low P_2O_5 fraction (max. ~3 mol%), the presence of phosphate units in the glass network is expected to be mainly under the form of isolated PO_4 tetrahedra (no pyrophosphate or P–O–P linkage), in analogy with phosphosilicate glasses [28]. Because phosphorus is completely miscible in silica, the P^{5+} cations require the formation of a terminal P=O bond which destroys the 3D fully connected network of SiO_2 creating non-bridging oxygen [7]. Al_2O_3 behaves as a network modifier and the Al^{3+} ions are connected to the NBO atoms of the network, like in silicate and borosilicate glasses for low Al content [29]. The introduction of P_2O_5 or Al_2O_3 in the glass matrix is expected to lead to the formation of negatively-charged PO_4 or AlO_4 units but also to Si-O-Al, P-O-Al and Si – O – P stretch as revealed by the presence of broad band in the 1000-1200 cm^{-1} range [28]. The presence of this broad band suggests that

an interconnected Si–O–Al/ Si-O-P network is formed upon Al_2O_3 and P_2O_5 addition rather than formation of SiO_2- and Al_2O_3/P_2O_5-rich regions in the sol-gel powders. Therefore, the network of the sol-gel with x=0.3 is suspected to be formed by a large number of Si-NBO induced by the presence of PO_4 units as confirmed by presence of the bands in the 1000-1300cm^{-1}. An increase in x from 0.3 to 3.3 leads to an increase in the intensity of the bands at 485 and 600cm^{-1} indicating that an increase in Al_2O_3 at the expense of P_2O_5 leads to changes in the ring distribution. When x increases to 1, the number of PO_4 units is expected to be reduced due to the progressive formation of $AlPO_4$ units as seen by the appearance of the shoulder at 1144cm^{-1} which was attributed to [$AlPO_4$] [10]. As explained in [7], the formation of $AlPO_4$ units restores the 3D network by replacing an O=P non-bridging oxygen bond with an Al-O-P linkage between 2 tetrahedra. When x increases from 1 to 3.3, the number of $AlPO_4$ units decreases due to the formation of AlO_4 units leading to an increase in the number of Si-O-Al sites and thus to a depolymerization of the silica glass network. This change in the silica network dimensionality as a function of the x is confirmed by the increase in intensity of the band at 800cm^{-1} and in the 1000-1200 cm^{-1} when x increases from 0.3 to 1 and then by the decrease in intensity of those bands when x increases from 1 to 3.3. These changes in the network dimensionality are suspected to affect the visible and IR emission properties of Yb^{3+} as discussed earlier; the addition of Al_2O_3 at the expense of P_2O_5 promotes the formation of Yb^{2+} at the expense of Yb^{3+} as suggested in [10].

Finally, one can notice that the intensity of the bands at 600 and 980cm^{-1} increases with an increase of x indicating that the progressive replacement of P_2O_5 by Al_2O_3 increases the Si-OH content as suggested from the up-conversion emission spectra presented in Figure 5. It should be pointed out that, for some unknown reason, the spectrum of the sol-gel with x=1.25 exhibits those 2 bands with the largest intensity which could be related to a higher OH content in this sol-gel as compared to the other sol-gels.

Conclusion

Yb^{3+} doped P_2O_5-Al_2O_3-SiO_2 sol-gel powders were prepared with different compositions in order to investigate the real impact of the P_2O_5 and Al_2O_3 addition in silica network on the Yb^{3+} spectroscopic properties. We confirmed that an increase in the Al/P ratio leads to an increase in the Yb^{3+} emission at 1µm. At Al/P ratio=1, the network is suspected to be similar to that of pure SiO_2 due to the formation of $AlPO_4$ units. From the optical and luminescence properties of Yb^{3+}, Al and P have a noticeable impact on the crystallographic site of Yb^{3+} by modifying the coordination shell of Yb^{3+}. We found that an increase of SiO_2 has an impact on the Yb^{3+} emission properties and should be taken into account when studying the impact of the sol-gel composition on rare-earth spectroscopic properties. Finally, when investigating the Yb luminescence properties in different sol-gel glasses, it is crucial to compare the OH content in those sol-gels before comparing the Yb^{3+} emission.

Acknowledgements

The authors would like to acknowledge the financial support of the Academy of Finland through the Competitive Funding to Strengthen University Research Profiles program (310359). Mr. Mikael Moussa is thanked for carrying out photoluminescence and up-conversion luminescence measurements.

Reference

[1] J. Limpert, T. Schreiber, S. Nolte, H. Zellmer, A. Tünnermann, R. Iliew, F. Lederer, J. Broeng, G. Vienne, A. Petersson, C. Jakobsen, “High-power air-clad large-mode-area photonic crystal fiber laser”, Optics Express,.11 (2003) 818-823

[2] A. Galvanauskas, “High Power Fiber Lasers”, Optics & Photonics News, 15 (2004) 42-47

[3] A. Langner, M. Such, G. Schötz, V. Reichel, S. Grimm, F, Just, M.Leich, J. Kirchhof, B. Wedel, G. Köhler, O. Strauch, O. Mehl, V. Krause, G. Rehmann, "Development, manufacturing and lasing behavior of Yb-doped ultra large mode area fibers based on Yb-doped fused bulk silica", Proceedings of SPIE, (2010) 75802X

[4] C. Ye, L. Petit, J. Koponen, I-N. Hu, A. Galvanauskas, "Short-term and long-term stability in ytterbium-doped high-power fiber lasers and amplifiers", IEEE Journal of Selected Topics in Quantum Electronics, 20 (2014) 903512

[5] K. Arai, H. Namikawa, K. Kumata, T. Honda Yoshiro Ishii, T. Handa, "Aluminum or phosphorus co-doping effects on the fluorescence and structural properties of neodymium-doped silica glass ", J. Appl. Phys. 59 (1986) 593430-3436

[6] M.E. Likhachev, M.M. Bubnov, K.V. Zotov, O.I. Medvedkov, D.S. Lipatov, M.V. Yashkov, A.N. Gur'yanov, "Erbium-doped aluminophosphosilicate optical fibres", Quant. Electr. 40 (2010) 633-638

[7] D.J. DiGiovanni, J.B. MacChesney, T.Y. Kometani, "Structure and properties of silica containing aluminum and phosphorus near the $AlPO_4$ join", J. Non-Cryst. Solids, 113 (1989) 58-64

[8] S. Jetschke, S. Unger, A. Schwuchow, M. Leich, J. Kirchhof, "Efficient Yb laser fibers with low photodarkening by optimization of the core composition", Opt. Express 16 (2008) 15540.

[9] C.J. Brinker and G.W. Scherer, Sol-Gel Science: The Physics and Chemistry of Sol-Gel Processing (Academic, New York, 1990)

[10] S. Wang, F. Lou, C. Yu, Q. Zhou, M. Wang, S. Feng, D. Chen, L. Hu, W. Chen, M. Guzik, "Influence of Al^{3+} and P^{5+} ion contents on the valence state of Yb^{3+} ions and the dispersion effect of Al^{3+} and P^{5+} ions on Yb^{3+} ions in silica glass", J. Mater. Chem. C 2 (2014) 4406.

[11] W. Xu, J. Ren, C. Shao, X. Wang, M. Wang, L. Zhang, D. Chen, S. Wang, C. Yu, L. Hu, "Effect of P^{5+} on spectroscopy and structure of $Yb^{3+}/Al^{3+}/P^{5+}$ co-doped silica glass", J. Luminesc, 167 (2015) 8–15

[12] H. Aguiar, J. Serra, P. González, B. León, "Structural study of sol–gel silicate glasses by IR and Raman spectroscopies ", J. Non-Cryst. Solids 355 (2009) 475–480

[13] A.Monteil, S. Chaussedent, G. Alombert-Goget, M. Gaumer. J. Obriot, S.J.L. Ribeiro, Y. Messaddeq, A. Chiasera, M. Ferrari "Clustering of rare earth in glasses, aluminium effect: experiments and modelling" J. Non-Crystalline Solids 348 (2004) pp. 44-50.

[14] Y. Qiao, L. Wen, B. Wu, J. Ren, D. Chen, J. Qiu, "Preparation and spectroscopic properties of Yb-doped and Yb-Al codoped high silica glasses", Materials Chemistry and Physics, 107 (2008) 488-491

[15] J. Petit, B. Viana, P. Goldner, "Internal temperature measurement of an Ytterbium doped material under laser operation", Opt. Exp., 19 (2011) 1138-1146

[16] T. Deschamps, N. Ollier, H. Vezin, C. Gonnet, "Clusters dissolution of Yb^{3+} in codoped SiO_2-Al_2O_3-P_2O_5 glass fiber and its relevance to photodarkening", J. Chem. Phys., 136 (2012) 014503

[17] F. Auzel, "Upconversion and Anti-Stokes Processes with f and d Ions in Solids", Chem. Rev., 104 (2004) 139−173

[18] V. Jubera, A. Garcia, J.P. Chaminade, F. Guillen, J. Sablayrolles, C. Fouassier, « Yb^{3+} and Yb^{3+}-Eu^{3+} luminescent properties of the $Li_2Lu_5O_4(BO_3)_3$ phase", J. Lumin., 124 (2007) 10-14

[19] B. D.White, L. J. Brillson, M. Bataiev, L. J. Brillson, D. M. Fleetwood, R. D. chrimpf, B. K. Choi, D. M. Fleetwood, S. T. Pantelides, "Detection of trap activation by ionizing radiation in SiO_2 by spatially localized cathodoluminescence spectroscopy", J. Appl. Phys. 92 (2002) 5729

[20] H. Yang, X. Yao, D. Huang, ”Sol–gel synthesis and photoluminescence of AlP nanocrystals embedded in silica glasses”, Opt. Mat., 29 (2007) 747-752

[21] D. Feng, Q. He, M. Lu, W. Li, W. Song, P. Wang, B. Peng, “Investigations on the photoluminescence spectra and its defect-related nature for the ultraviolet transmitting fluoride-containing phosphate-based glasses”, J. Non-Cryst. Solids, 425 (2015) 130-137

[22] J. Gotze, M. Plotze, D. Habermann, “Origin, spectral characteristics and practical applications of the cathodoluminescence (CL) of quartz – a review.”, Mineralogy and Petrology, 71 (2001) 225-250

[23] V. B. Mikhailik, P. C. F. Di Stefano,. S. Henry, H. Kraus, A. Lynch, V. Tsybulskyi, M. A. Verdier, “Studies of concentration dependences in the luminescence of Ti-doped Al_2O_3”, Journal of Applied Physics, 109 (2011) 053116

[24] R.J. Bell, N.F. Bird, P. Dean, “The vibrational spectra of vitreous silica, germania and beryllium fluoride“, J. Phys. C 1 (1968) 299.

[25] F.L. Galeener, “Band limits and the vibrational spectra of tetrahedral glasses”, Phys. Rev. B 19 (1979) 4292.

[26] M.J. Matthews, A. L. Harris, A. J. Bruce, M. J. Cardillo, “Characterization of phosphosilicate thin films using confocal Raman microscopy”, Review of Scientific Instruments 71, (2000) 2117-2120

[27] T.V. Ribeiro, L.F. Santos, M.C. Goncalves, R.M. Almeida, “Heavily Yb-doped silicate glass thick films”, J. Sol-Gel Sci. Technol. DOI 10.1007/s10971-016-4071-7

[28] V.G. Plotnichenko, V.O. Sokolov, V.V. Koltashev, E.M. Dianov, “On the structure of phosphosilicate glasses”, J. Non-Cryst. Solids 306 (2002) 209–226

[29] E.I. Kamitsos, J.A Kapoutsis, H. Jain, H.S. Hsieh, “Vibrational study of the role of trivalent ions in sodium trisilicateglass”, J. Non-Cryst. Solids, 172 (1994) 31-45.

TABLE CAPTIONS

Table 1: Composition of the investigated samples (mol%)

FIGURE CAPTIONS

Figure 1: Normalized emission band under 980nm of the sol-gels with x=1.25 (a) and intensity of the emission at 1000nm under 980nm excitation as a function of SiO_2 mol% in sol-gels with x=0.8 and 1.25 (b)

Figure 2: Up-conversion emission spectra under 974nm excitation as a function of SiO_2 mol% in sol-gels with x=0.8 (a) and 1.25 (b)

Figure 3: Photoluminescence emission spectra of the investigated samples as a function of SiO_2 mol% in sol-gels with x=0.8 (a) and 1.25 (b) (λ_{exc}=255nm)

Figure 4: Intensity of the emission at 1µm under 980nm excitation (a) and normalized emission band under 250nm excitation (b) as a function of x

Figure 5: Up-conversion emission spectra of the investigated samples as a function of x (λ_{exc}=974nm)

Figure 6: Photoluminescence emission spectra of the investigated samples as a function of x (λ_{exc}=255nm)

Figure 7: Raman spectra of the investigated samples as a function of x

Table 1: Composition of the investigated samples (mol%)

mol%				x (Al/P)
SiO_2	**Al_2O_3**	**P_2O_5**	**Yb_2O_3**	
95.8	0.92	3.08	0.2	0.3
95.8	1.78	2.22	0.2	0.8
95.8	2	2	0.2	1.0
95.8	2.22	1.78	0.2	1.25
95.8	3.08	0.92	0.2	3.3
91.8	3.56	4.44	0.2	0.8
97.8	0.89	1.11	0.2	0.8
91.8	4.44	3.56	0.2	1.25
97.8	1.11	0.89	0.2	1.25

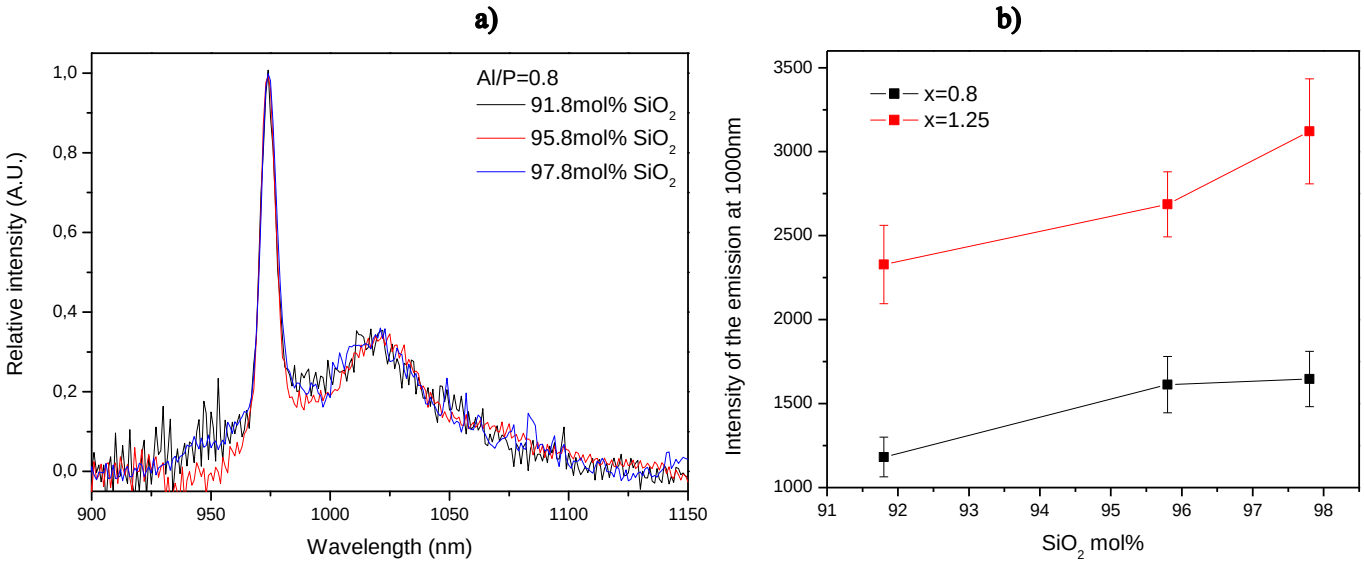

Figure 1: Normalized emission band under 980nm of the sol-gels with x=1.25 (a) and intensity of the emission at 1000nm under 980nm excitation as a function of SiO_2 mol% in sol-gels with x=0.8 and 1.25 (b)

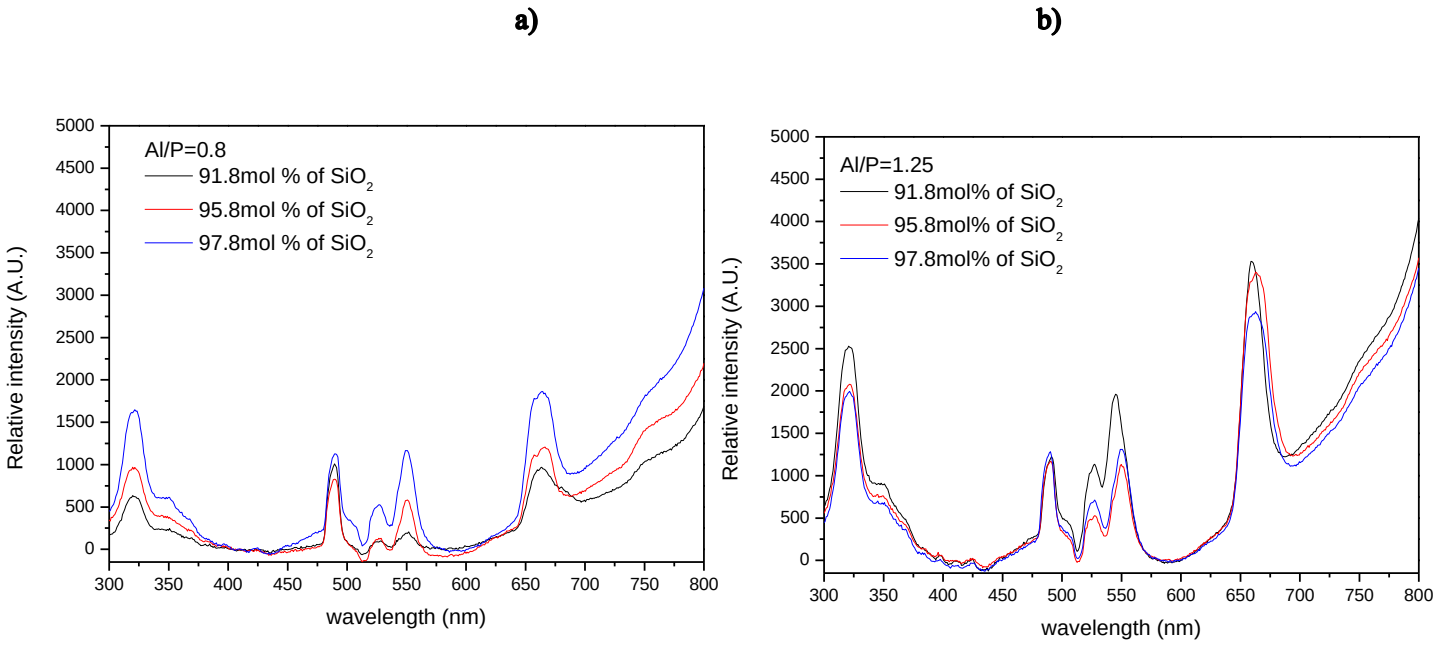

Figure 2: Up-conversion emission spectra under 974nm excitation as a function of SiO_2 mol% in sol-gels with x=0.8 (a) and 1.25 (b)

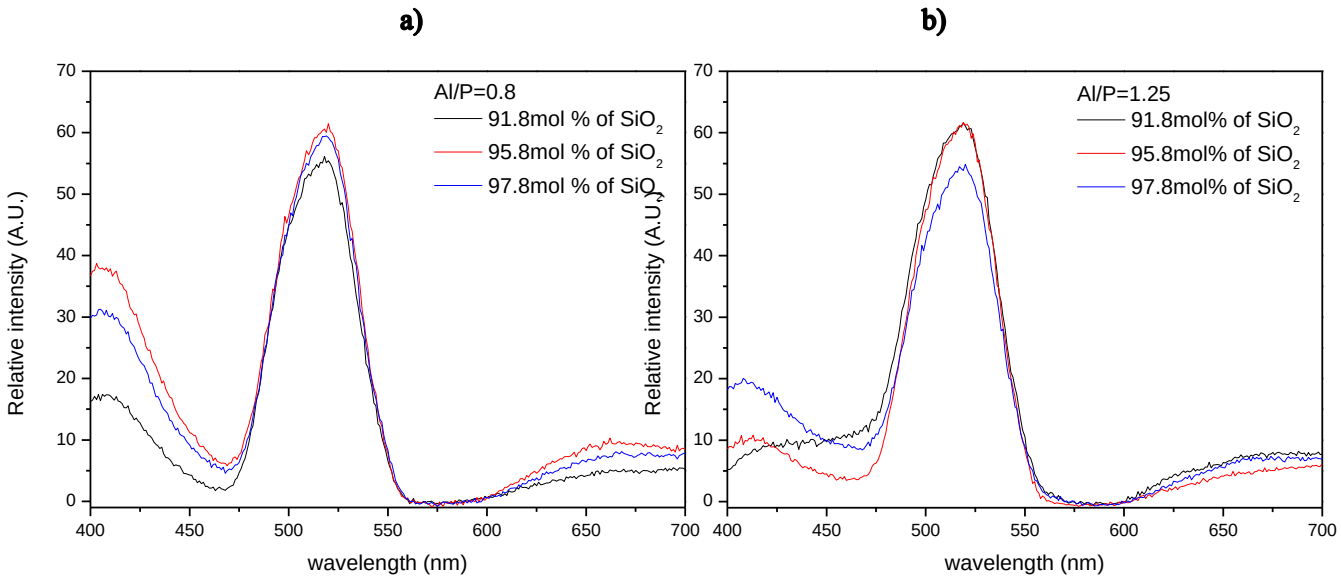

Figure 3: Photoluminescence emission spectra of the investigated samples as a function of SiO_2 mol% in sol-gels with x=0.8 (a) and 1.25 (b) (λ_{exc}=255nm)

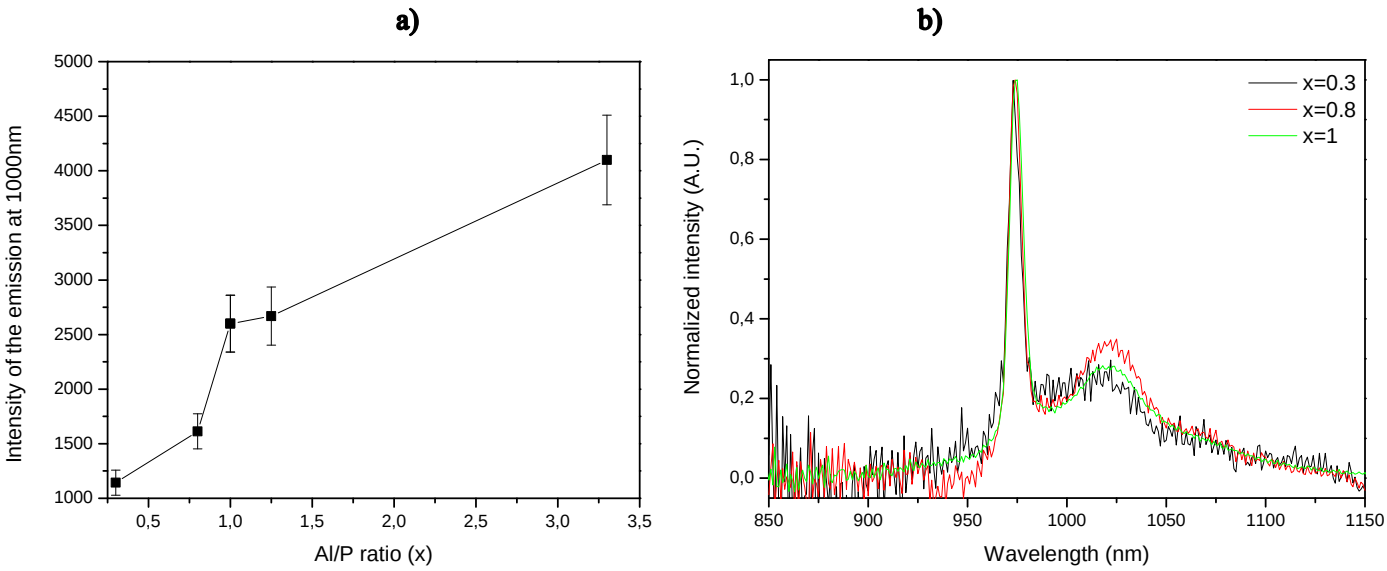

Figure 4: Intensity of the emission at 1µm under 980nm excitation (a) and normalized emission band under 250nm excitation (b) as a function of x

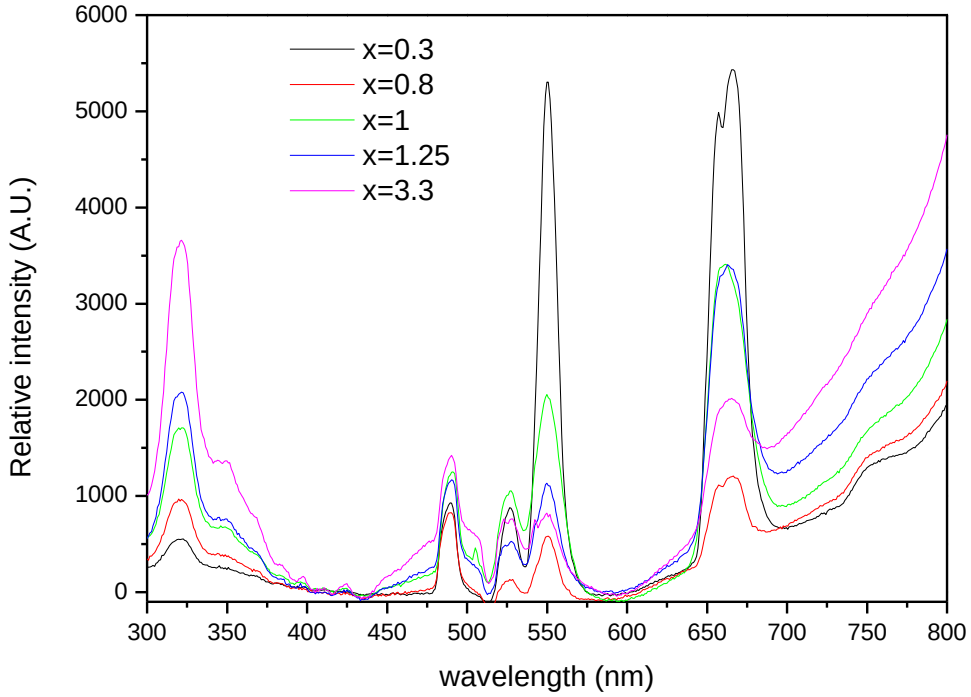

Figure 5: Up-conversion emission spectra of the investigated samples as a function of x (λ_{exc}=974nm)

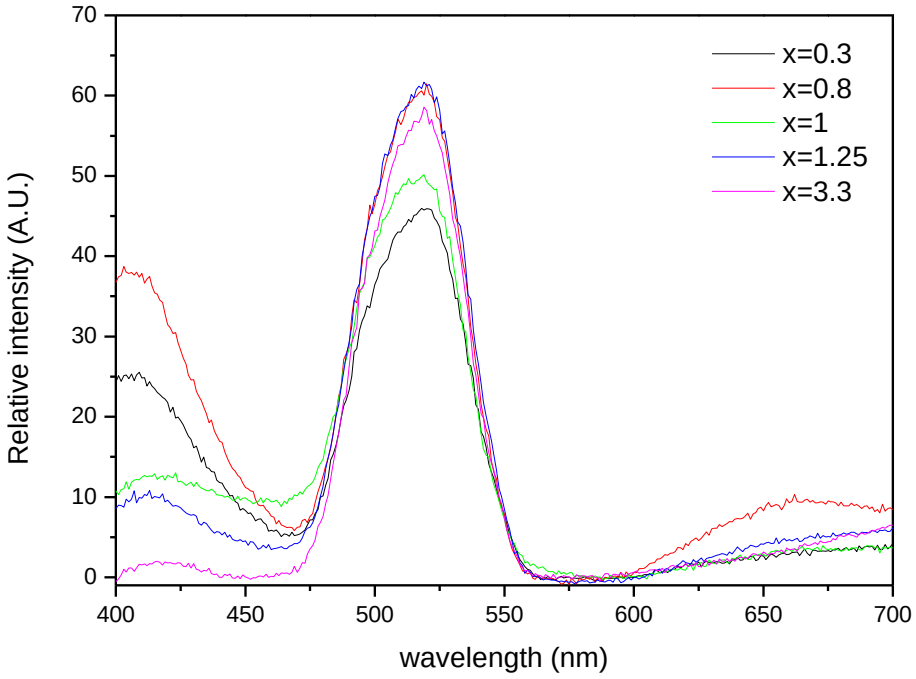

Figure 6: Photoluminescence emission spectra of the investigated samples as a function of x (λ_{exc}=255nm)

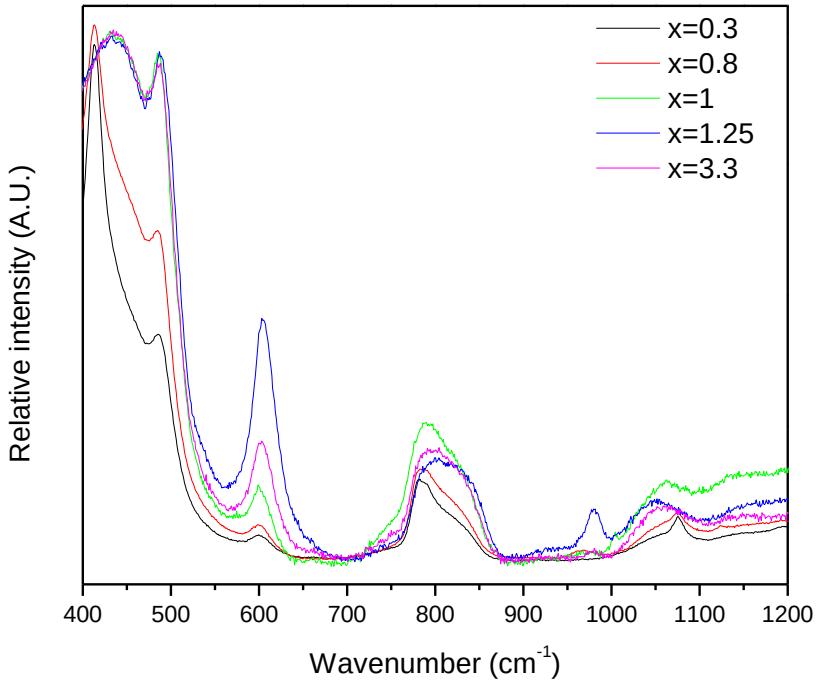

Figure 7: Raman spectra of the investigated samples as a function of x